Organic & Biomolecular Chemistry

ROYAL SOCIETY OF CHEMISTRY

PAPER

View Article Online
View Journal | View Issue

Cite this: *Org. Biomol. Chem.*, 2025, **23**, 8012

Interplay between molecular recognition and acid–base reactivity in tailored metal-based calix[6]arene receptors

Martin Lepeintre,[a,b] Aleksandar Višnjevac,[c] Ivan Jabin *[a] and Benoit Colasson *[b]

Received 7th July 2025,
Accepted 28th July 2025

DOI: 10.1039/d5ob01099c

rsc.li/obc

This study explores the interplay between molecular recognition and acid–base reactivity in two novel Zn–calix[6]arene funnel complexes featuring phenol units in place of the anisole units present in the parent systems. The two complexes differ in the accessibility of their third coordination sphere. NMR and X-ray crystallography revealed that, like their anisole-based predecessors, these new complexes can encapsulate neutral guests such as acetonitrile. However, in contrast to the parent systems, which strongly bind primary amines, the new phenol-based systems undergo a base-induced structural reorganization upon addition of propylamine, triggered by a selective metal-assisted phenol deprotonation. Moreover, the presence of phenol groups enables intra–cavity binding of anions, provided their structure allows for simultaneous stabilization through hydrogen bonding. Finally, differences in the accessibility of the third coordination sphere between the two complexes influenced their affinity for long linear anions. These findings underscore a delicate balance between coordination–driven recognition, hydrogen bonding, and acid–base chemistry in such systems. The work expands the understanding of first, second and third coordination sphere effects in metallo–receptors and demonstrates how subtle structural modifications can modulate binding modes. It also suggests new directions for designing responsive host systems capable of switching behavior under mild stimuli.

Introduction

Molecular recognition plays a pivotal role in many biological processes, including enzymatic catalysis,[1,2] signal transduction[3] and allosteric regulation.[4,5] The exquisite selectivity of biological receptors largely stems from multipoint recognition, whereby spatially organized interactions achieve high complementary with the target substrate. Artificial receptors were primarily designed to gain insight into the fundamental principles of molecular recognition processes[6] and have since found applications in catalysis,[7–9] sensing,[10–14] molecular transport,[15,16] and drug design.[17–20] To achieve the level of selectivity observed in biological receptors, a strategy relies on the use of artificial receptors based on macrocyclic concave platforms (*eg*, cucurbiturils,[21] cyclodextrines,[22] resorcinarenes,[23–25] pillararenes,[26–28] calixarenes,[29] and others[30–33]) bearing functional groups capable of engaging in diverse non-covalent interactions. Among these, cavitands have been combined with metal complexes to design metallo-based receptors, where synergistic effects between the metal coordination site and the molecular cavity were observed.[34–39] The potential applications of such receptors can be finely tuned by modifying the metal ion, its first and second coordination spheres,[40] or even more distal regions of the receptor (third coordination sphere).

Calix[*n*]arenes[29] offer a particularly attractive scaffold for designing such receptors due to their tunable cavity,[41] which enables selective binding of guest molecules through tailored non-covalent interactions.[42] Over the past several years, we have been working on calix[6]arenes as promising platforms for designing funnel-shaped complexes that emulate metalloenzymatic active sites.[35,43,44] By anchoring aza-coordinating units at the narrow rim of calix[6]arenes, it generates a cavity-based receptor with a deeply embedded metal center that mimics the binding pockets of metalloenzymes. The funnel complexes were explored within the framework of host–guest chemistry, focusing on their ability to interact selectively with various neutral molecules.[45,46] Calixarene-based funnel complexes can be classified into two main generations: (i) first-generation complexes, in which the metal ion is coordinated

[a]*Laboratoire de Chimie Organique, Université libre de Bruxelles (ULB), Avenue F.D. Roosevelt 50, CP160/06, B-1050 Brussels, Belgium. E-mail: Ivan.Jabin@ulb.be*
[b]*Université Paris Cité, CNRS, Laboratoire de Chimie et de Biochimie Pharmacologiques et Toxicologiques, F-75006 Paris, France. E-mail: benoit.colasson@u-paris.fr*
[c]*Ruđer Bošković Institute, Physical Chemistry Division, Bijenička 54, HR-10000 Zagreb, Croatia*

by three independently grafted N-ligands (*e.g.* imidazole groups, see ligand **1** in Fig. 1),[47] and (ii) second-generation complexes, where the metal ion is coordinated by a grafted polydentate N-ligand such as TREN (tris(2-aminoethyl) amine)[48] or TMPA (tris(2-pyridylmethyl)amine)[49] (see ligands **Calix-TMPA^{Y}** and **Calix-Tren^{Y}** in Fig. 1). With the exception of Calix-TMPA-based receptors,[50] these funnel complexes do not bind anions. This reluctance for anions arises from the conformation of the complexes: the oxygen atoms at the narrow rim are oriented such that their lone pairs point inward, creating an electrostatically repulsive environment for negatively charged species. We recently modified the second coordination sphere of the second-generation complexes by replacing the three anisole units with phenol ones (see inset Fig. 1 for the representation of coordination spheres).[51] This alteration had a significant impact on the host–guest properties of the receptors, inducing a conformational change at the level of the second coordination sphere and enabling the intracavity binding of anions.[52,53] Specifically, the steric relief at the narrow rim allowed the lone pairs of the oxygen atoms to orient outward, thereby reducing electrostatic repulsion and facilitating hydrogen bonding between the phenol groups and the encapsulated anion. However, the synthetic strategy to remove the methoxy groups at the narrow rim (*i.e.* use of trimethylsilyl iodide) is incompatible with the presence of (Het) $ArCH_2$ groups and thus with the first-generation systems. Recently, we reported a new synthetic route leading to calix[6]arene-trisimidazole-based ligands (**2** and **3**) presenting three phenol units.[54] This strategy involves an iteroselective and regioselective 1,3,5-tris protection of the phenol units with allyl groups, followed by introduction of the imidazole units and removal of the allyl protecting groups through a Tsuji–Trost reaction (Scheme 1). Similarly to what was observed for the second-generation systems, we anticipated that the corresponding metal complexes would exhibit interesting host–guest properties toward H-bond acceptor guests such as anions.

In this study, we report two novel first-generation calix[6]arene-based zinc complexes featuring three phenol units in

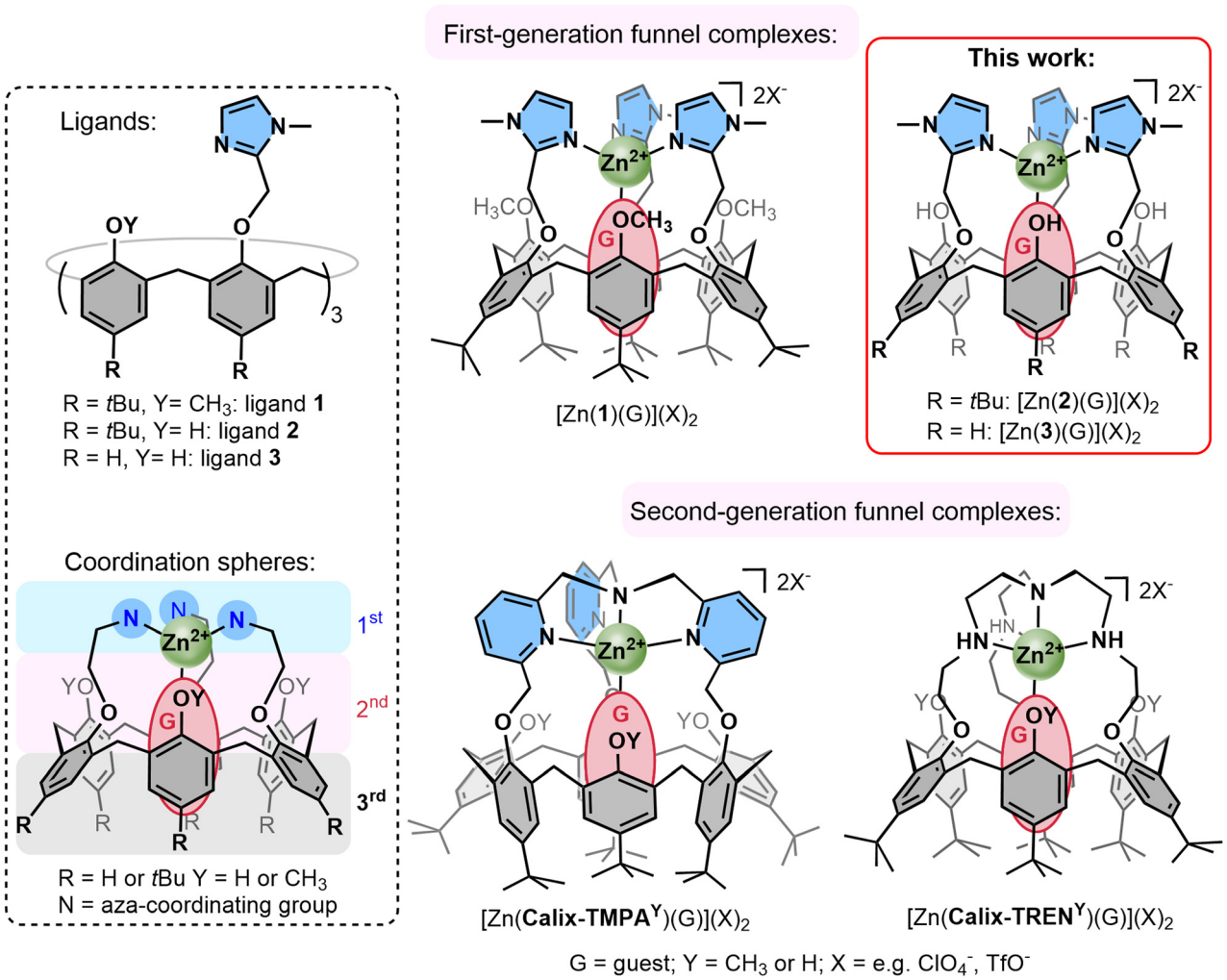

Fig. 1 Presentation of the two generations of funnel complexes and the complexes discussed in this work. Inset: general structure of ligands **1**, **2** and **3** (top), schematic representation of the three coordination spheres (bottom).

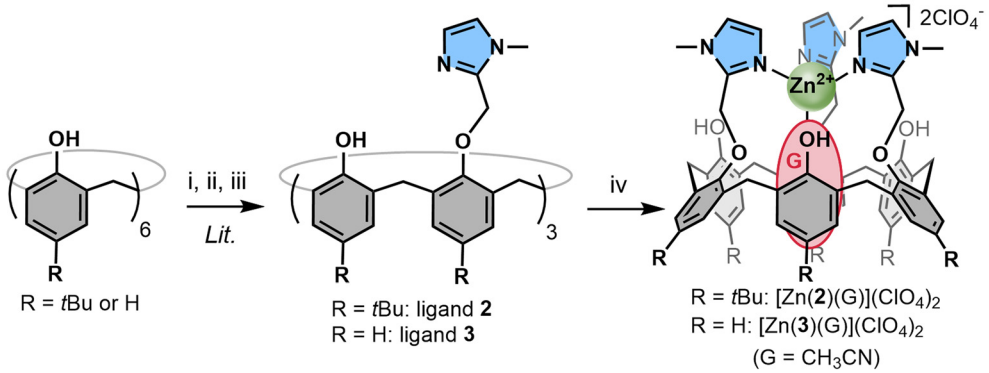

Scheme 1 Synthesis of $[Zn(\mathbf{2})(G)](ClO_4)_2$ and $[Zn(\mathbf{3})(G)](ClO_4)_2$. (i) K_2CO_3, allylbromide, acetone, reflux. (ii) 2-(Chloromethyl)-1-methyl-1*H*-imidazole hydrochloride, NaH, THF_{anh}/DMF_{anh} 8 : 2, reflux; (iii) $Pd(OAc)_2$, PPh_3, Et_2NH, THF/H_2O 87 : 13, reflux. Ligands **2** and **3** were obtained in 23% and 22% overall yields, respectively.[54] (iv) $Zn(H_2O)_6(ClO_4)_2$, acetonitrile/chloroform, rt, 1 h, 87% and 90% for zinc complexes isolated from **2** and **3**, respectively.

their second coordination sphere. These complexes differ in cavity accessibility (third coordination sphere), determined by the presence (ligand **2**) or absence (ligand **3**) of *t*Bu groups on the large rim of the calixarene (Fig. 1). Their host–guest behaviour was examined and compared to that of the parent complex obtained with ligand **1**. A combination of studies by NMR spectroscopy and X-ray crystallography revealed a strong entanglement between molecular recognition and acid–base behaviour in these biomimetic receptors, governed by the multiple levels of interaction provided by their architectures.

Results and discussion

Synthesis and characterization of $[Zn(\mathbf{2})(G)](ClO_4)_2$ and $[Zn(\mathbf{3})(G)](ClO_4)_2$

Ligands **2** and **3** were synthesized using a three-step iteroselective approach recently developed by our group (Scheme 1).[54] The corresponding zinc complexes $[Zn(\mathbf{2}$ or $\mathbf{3})(G)](ClO_4)_2$ (G stands for a molecule of coordinating acetonitrile, *vide infra*) were prepared through the addition of 1 equiv. of $Zn(H_2O)_6(ClO_4)_2$ to a 1 : 1 $CH_3CN/CHCl_3$ solution containing the ligand. Precipitation with Et_2O and filtration of the solid afforded the pure complexes in high yield.

The ^{1}H NMR spectra of complexes $[Zn(\mathbf{2})(G)](ClO_4)_2$ and $[Zn(\mathbf{3})(G)](ClO_4)_2$ in $CD_3CN/CDCl_3$ (1 : 1) are consistent with an average C_{3v} symmetry (Fig. 2a and b). The spectrum of $[Zn(\mathbf{2})(G)](ClO_4)_2$ (Fig. 2b) is almost identical to that of the parent complex $[Zn(\mathbf{1})(G)](ClO_4)_2$, with the only notable difference being the absence of the OCH_3 resonance at 3.57 ppm (Fig. S2). A less symmetrical minor calixarene species can be also detected in the spectrum of $[Zn(\mathbf{2})(G)](ClO_4)_2$, notably through the presence of additional *t*Bu peaks at 1.38 and 0.87 ppm. ROESY experiments revealed exchange correlations between the peaks of this minor species and the major one, suggesting a dynamic equilibrium between conformers (Fig. S7 and S8). This minor species likely corresponds to a conformer of $[Zn(\mathbf{2})(G)](ClO_4)_2$ with one or two inverted phenolic units. For both complexes $[Zn(\mathbf{2})(G)](ClO_4)_2$ and $[Zn(\mathbf{3})(G)](ClO_4)_2$, HMBC and HSQC NMR experiments confirmed that the calixarene adopts a flattened cone conformation, in which the phenol units are pinched at the large rim, as the anisole units are in the parent complex (Fig. S5, S6, S15 and S16). The phenolic OH signals of these two complexes were identified *via* D_2O exchange experiments (Fig. S9 and S17). Addition of an excess of non-deuterated acetonitrile (100 µl) to each complex resulted in the appearance of a new high-field singlet below 0 ppm, showing the intracavity coordination of a CH_3CN molecule and confirming that a molecule of CD_3CN was already coordinated within the cavity prior to CH_3CN addition (Fig. S10 and S18). The complexation-induced shifts (CIS = $\delta_{bound} - \delta_{free}$) for CH_3CN are −2.56 ppm for $[Zn(\mathbf{2})(CH_3CN)](ClO_4)_2$ in $CDCl_3$ and −2.00 ppm for $[Zn(\mathbf{3})(CH_3CN)](ClO_4)_2$ in $CDCN_3/CDCl_3$ 1 : 1. These values are comparable to that of the parent complex $[Zn(\mathbf{1})(CH_3CN)](ClO_4)_2$ in $CDCl_3$ (*i.e.* −2.76 ppm),[47] confirming a similar recognition mode across the three systems.

Single crystals suitable for X-ray diffraction were obtained by slow diffusion of methyl *tert*-butyl ether into a 1 : 1 acetonitrile/chloroform solution of $[Zn(\mathbf{3})(CH_3CN)](ClO_4)_2$ (Fig. 3 and Table S1). The Zn(II) center resides within a tetrahedral N_4 ligand environment, displaying a non-crystallographic C_3 symmetry. The three imidazole arms wrap around the metal center in a chiral propeller-like arrangement, with an average Zn–N distance of 1.98 Å. The acetonitrile molecule provides the fourth N-ligand [*d*(Zn–N) = 2.01 Å] and is deeply embedded within the cavity of the calix[6]arene macrocycle. The calix[6]arene adopts a flattened cone conformation. The phenol units are oriented outward, with their OH groups pointing away from the cavity, while the OCH_2-imidazole moieties are oriented inward, pointing the lone pairs of the oxygen atoms toward the metal cation. All these data are in full agreement with what was observed in solution by NMR spectroscopy. Notably, both perchlorate counterions are positioned at H-bond distances from the hydroxyl groups of two phenol units (O···O distances of 2.86 Å and 2.90 Å).

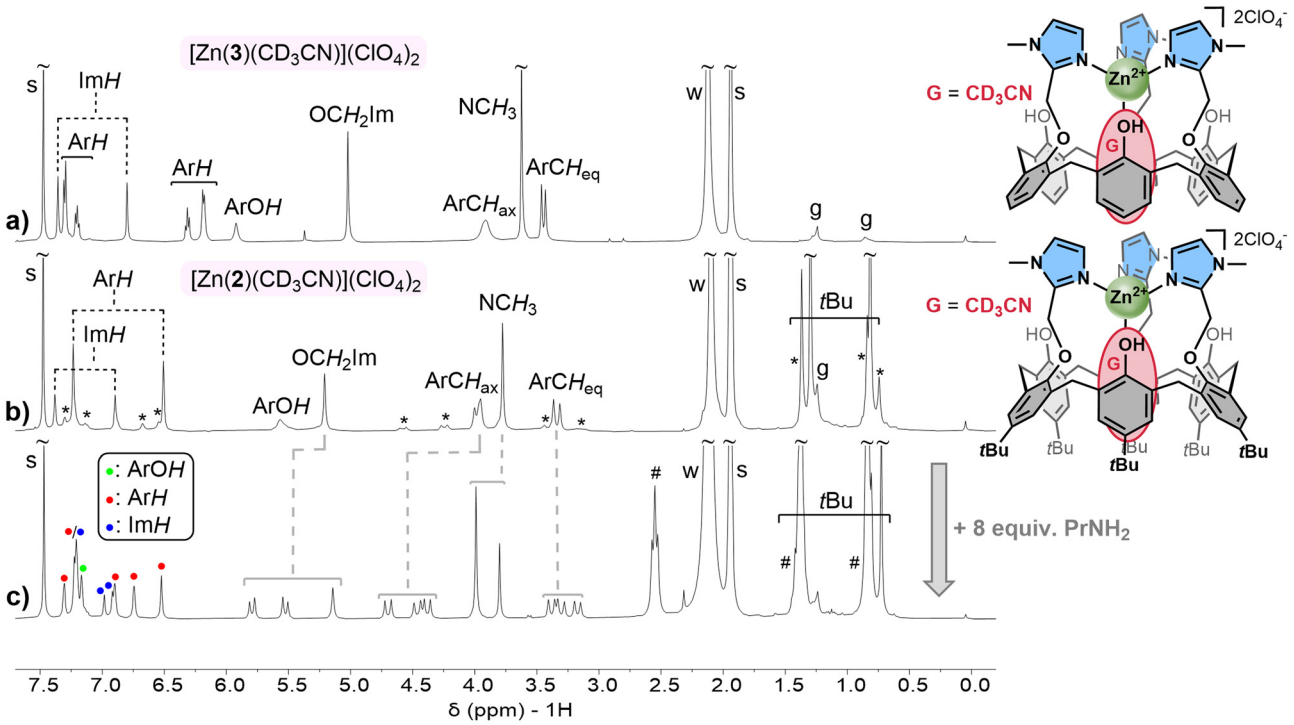

Fig. 2 ^{1}H NMR spectra (298 K, $CD_3CN/CDCl_3$ 1 : 1) of (a) [Zn(**3**)(CD_3CN)](ClO$_4$)$_2$; (b) [Zn(**2**)(CD_3CN)](ClO$_4$)$_2$; (c) [Zn(**2**)(G)](ClO$_4$)$_2$ with 8 equiv. of propylamine. Spectra were recorded at either 400 MHz (a) or 500 MHz (b and c). S: solvent, w: water, g: grease. *: minor conformer. #: free $PrNH_2$.

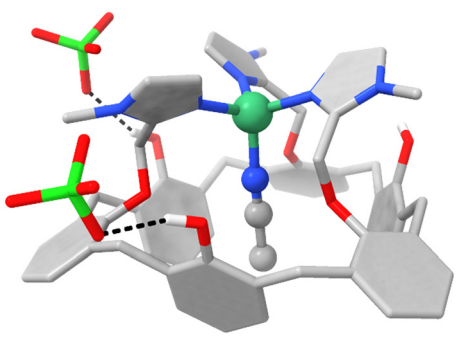

Fig. 3 X-ray diffraction structure of [Zn(**3**)(CH_3CN)](ClO$_4$)$_2$. H-bonds are indicated by black dashed lines.

Taken together, the data from both solution and solid-state analyses indicate that the new complexes [Zn(**2** or **3**)(G)](ClO$_4$)$_2$ exhibit similar host–guest properties as the parent complex [Zn(**1**)(G)](ClO$_4$)$_2$ toward neutral guests such as acetonitrile.

Host–guest properties toward basic neutral guests

First, the binding properties of [Zn(**2**)(G)](ClO$_4$)$_2$ and [Zn(**3**)(G)](ClO$_4$)$_2$ toward small neutral guests such as ethanol, DMF or benzonitrile were evaluated by ^{1}H NMR spectroscopy in $CDCl_3$/CD_3CN (1 : 1). The spectra of both zinc complexes remained unaffected upon the addition of a few equivalents of these molecules. This result is in line with the one previously reported for related funnel complexes, for which only primary amines (strong σ-donors) were able to displace the acetonitrile coordinated within the cavity.[47] The progressive addition of propylamine (up to 8 equiv.) to [Zn(**2**)(G)](ClO$_4$)$_2$ induced significant changes in its ^{1}H NMR spectrum (Fig. S19), in accordance with the formation of new species (Fig. 2c and S20). Two new slightly different NMR signatures could be identified over the course of the titration. For both species, the number of resonances indicates calixarene-based complexes with C_s symmetry. The first species exhibited broad signals and was obtained quantitatively after the addition of one equiv. of propylamine, while the second species exhibited sharp signals and was quantitatively obtained after the addition of 2 equiv. of amine. Full assignment of the ^{1}H signals of this latter species was achieved *via* HSQC, COSY and HMBC NMR experiments (Fig. S22–S24). The initial NC*H*$_3$ singlet at 3.77 ppm splits into two singlets at 3.99 ppm and 3.80 ppm in a 2 : 1 ratio. Additionally, the ArC*H* doublets at 3.96 ppm (H_{ax}) and 3.35 ppm (H_{eq}) split into three pairs of doublets. Also, the initial singlet at 5.00 ppm for the OC*H*$_2$ splits into two doublets (5.79 and 5.53 ppm) and one singlet (5.14 ppm) in a 1 : 1 : 1 ratio. All these changes are consistent with a symmetry reduction from C_{3v} to C_s. Unlike the parent complex [Zn(**1**)(G)](ClO$_4$)$_2$, no high-field signals indicative of propylamine inclusion were detected, suggesting an alternative binding mode. Similar changes were observed for [Zn(**3**)(G)](ClO$_4$)$_2$ upon addition of propylamine (*e.g.* the splitting of the OC*H*$_2$ singlets in three distinct signals) but, due to the higher flexibility of the deterbutylated calixarene scaffold, broad ^{1}H NMR

signals were observed along the whole titration, preventing a full assignment of the signals (Fig. S28 and S29).

We hypothesized that, in contrast to the parent zinc complex, the behaviour of complexes [Zn(**2**)(G)]$(ClO_4)_2$ and [Zn(**3**)(G)]$(ClO_4)_2$ was due to a preferential deprotonation of one of the phenol units by the basic amine, rather than intracavity coordination of this guest. Despite the C_s symmetry of the complex, only one ArO*H* resonance was identified at 7.16 ppm in the case [Zn(**2**)(G)]$(ClO_4)_2$, supporting this hypothesis (Fig. 2c). To test this hypothesis, a titration experiment was conducted with [Zn(**2**)(G)]$(ClO_4)_2$, using a bulkier and stronger organic base, *i.e.* 1,8-diazabicyclo(5.4.0)undec-7-ene (DBU). Compared to propylamine, similar shifts and splitting patterns (*e.g.* for OCH_2, ArCH_2) were observed upon DBU addition, indicating analogous structural changes (Fig. S25). First, broad NMR signals were observed and then a NMR signature only slightly distinct from that obtained with propylamine was obtained after the addition of 8 equiv. of DBU (Fig. S26). This suggests the formation of a very similar C_s-symmetrical complex only differing by the nature of an *exo*-coordinated ligand. Interestingly, when DBU was added to a solution of free ligand **2**, no modification was observed in the ^{1}H NMR spectrum, indicating that the deprotonation of **2** did not occur in absence of Zn^{2+} (Fig. S27).

All these data support a metal-assisted deprotonation of a phenol unit and that the resulting phenolate coordinates intramolecularly to the metal center in place of one imidazole unit (Scheme 2), yielding a C_s-symmetrical monocationic complex. This base-induced reorganization of the coordination environment disrupts the typical host–guest behaviour of funnel complexes, as it likely precludes intracavity binding by orienting the fourth coordination site outward, toward the bulk solvent. In this configuration, an external ligand (L = solvent, H_2O, propylamine, DBU, *etc.*) completes the coordination sphere. In summary, upon addition of 1 equiv. of base (propylamine or DBU), an acetonitrile molecule is likely *exo*-coordinated. Upon further base addition, the *exo*-position is then likely occupied by the base itself.

Single crystals of the complex [Zn(**3**)(G)]$(ClO_4)_2$ in the presence of 4 equiv. of propylamine were obtained by slow diffusion of diethyl ether into a 1 : 1 acetonitrile/chloroform solution of the complex (Fig. 4 and Table S1). XRD analysis confirmed the formation of a monocationic complex in which the metal center is bound in a tetrahedral geometry to the phenolate group [*d*(Zn–O) = 1.89 Å] and two imidazole units from the same ligand, the fourth coordination site being directed outward from the cavity. In the absence of a suitable exogenous ligand in the solid state, likely due to the volatility of both solvent molecules and propylamine, the *exo*-position is occupied by the remaining imidazole group of another ligand, leading to the formation of a coordination polymer. A perchlorate anion is H-bonded to the two remaining phenol groups of the calix[6]arene [*d*(O–O) = 2.85 and 2.90 Å] and balances, together with the coordinated phenolate, the +2 charge of the zinc cation. The cavity is hosting a non-coordinated acetonitrile molecule. The C_s symmetry of the complex deduced from the NMR study in solution is retained in the solid state for the monomeric complex. Altogether, this XRD analysis fully supports the conclusions drawn from the NMR

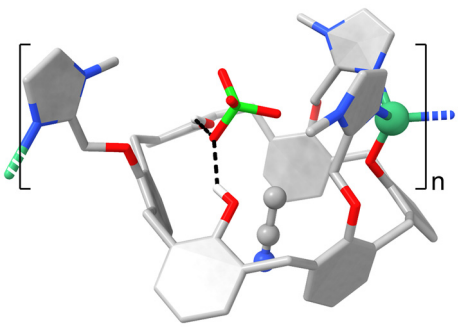

Fig. 4 X-ray diffraction structure obtained from [Zn(**3**)(CH_3CN)]$(ClO_4)_2$ in the presence of propylamine. H-bonds are indicated by black dashed lines. Square brackets and dashed bonds are used to define the coordination polymer.

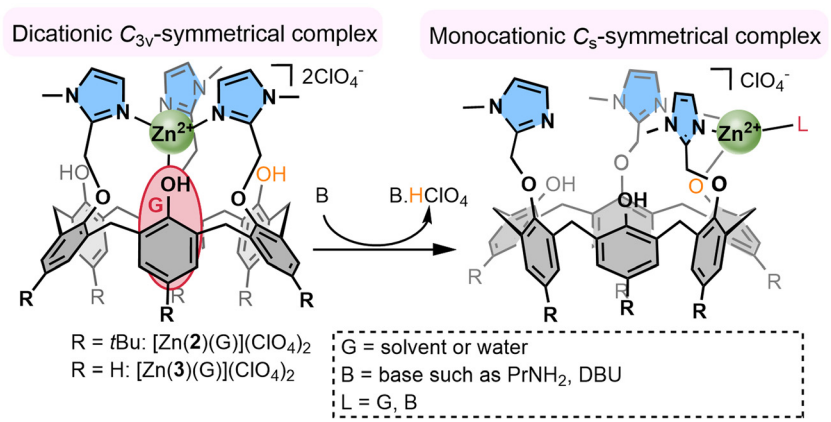

Scheme 2 Formation of a monocationic C_s-symmetrical complex through deprotonation of one of the phenol unit.

study in solution, highlighting that, in the presence of basic guests such as amines, acid–base reactivity takes the step on coordination chemistry, resulting in a significant alteration of the expected host–guest properties.

Host–guest properties toward anions

The parent complex $[Zn(\mathbf{1})(G)](ClO_4)_2$ is reluctant to host anions.[45] As mentioned above, the replacement of the three anisole units by phenol ones not only restores some conformational flexibility but also introduces H-bond donor sites. This modification should potentially enable the complexes $[Zn(\mathbf{2})(G)](ClO_4)_2$ and $[Zn(\mathbf{3})(G)](ClO_4)_2$ to function as anion receptors. To probe this hypothesis, the binding of acetate was first examined. A ^{1}H NMR titration of $[Zn(\mathbf{2})(G)](ClO_4)_2$ with tetrabutylammonium acetate (TBAOAc) was carried out in $CDCl_3$/CD_3CN (1 : 1). The titration showed the successive formation of two new species (Fig. 5, S30 and S31). From 0 to 1 equiv. of TBAOAc, a resonance at −0.80 ppm appeared and increased (Fig. 5b). After 1 equiv., the intensity of this resonance started to decrease and the rest of the spectrum became characteristic of the formation of a C_s-symmetrical complex (Fig. 5c). The three discrete species involved in this titration are in slow exchange on the NMR chemical shift timescale. The spectrum recorded with 1 equiv. of TBAOAc was further analysed by ^{1}H, ^{13}C and 2D NMR (Fig. S32–S36), allowing full assignment of the resonances (Fig. 5). The high-field signal (δ = −0.80 ppm) integrating for 3H was attributed to the methyl group of an acetate anion coordinated to the Zn^{2+} center within the cavity, forming the monocationic complex $[Zn(\mathbf{2})(OAc)](ClO_4)$. The CIS value for the acetate methyl group (−2.57 ppm) is similar to the one found for the coordinated CH_3CN (*vide supra*). Interestingly, while $[Zn(\mathbf{2})(OAc)](ClO_4)$ maintains an average C_{3v} symmetry and the classical flattened-cone conformation of the calix[6]arene framework, a conformational rearrangement occurs upon the intra-cavity coordination of the acetate (see structures displayed in Fig. 5a and b). This rearrangement was evidenced by an HMBC experiment (Fig. S36) and involves an *in–out* flip of the aromatic units, resulting in the reorientation of the three phenol OH groups toward the cavity. This conformational shift of the aromatic units likely alleviates electrostatic repulsion between the lone pairs on the phenolic oxygen atoms and simultaneously enables hydrogen bonding with the coordinated acetate anion.

Single crystals of the complex hosting an acetate molecule $[Zn(\mathbf{2})(OAc)](ClO_4)$ were grown by slow diffusion of Et_2O into a $CHCl_3/CH_3CN$ solution of $[Zn(\mathbf{2})(CH_3CN)](ClO_4)_2$ in the presence of 1 equiv. of TBAOAc (Fig. 6 and Table S1). Due to the poor quality of the crystals, the structure is somewhat ill-refined and one of the two complexes present in the asymmetric unit is particularly disordered. Nevertheless, the XRD structure confirms the *endo*-complexation of an acetate anion. The analysis of the less disordered complex reveals important features. The three coordinated imidazole arms adopt a helical arrangement around the zinc center with bond distances d(Zn–N) = 1.99, 2.00 and 2.03 Å. The acetate ligand is coordinated to the metal center in a bidentate mode [d(Zn–O) = 2.07 and 2.48 Å]. The three phenol groups point in the direction of the coordination site and establish H-bonds with the

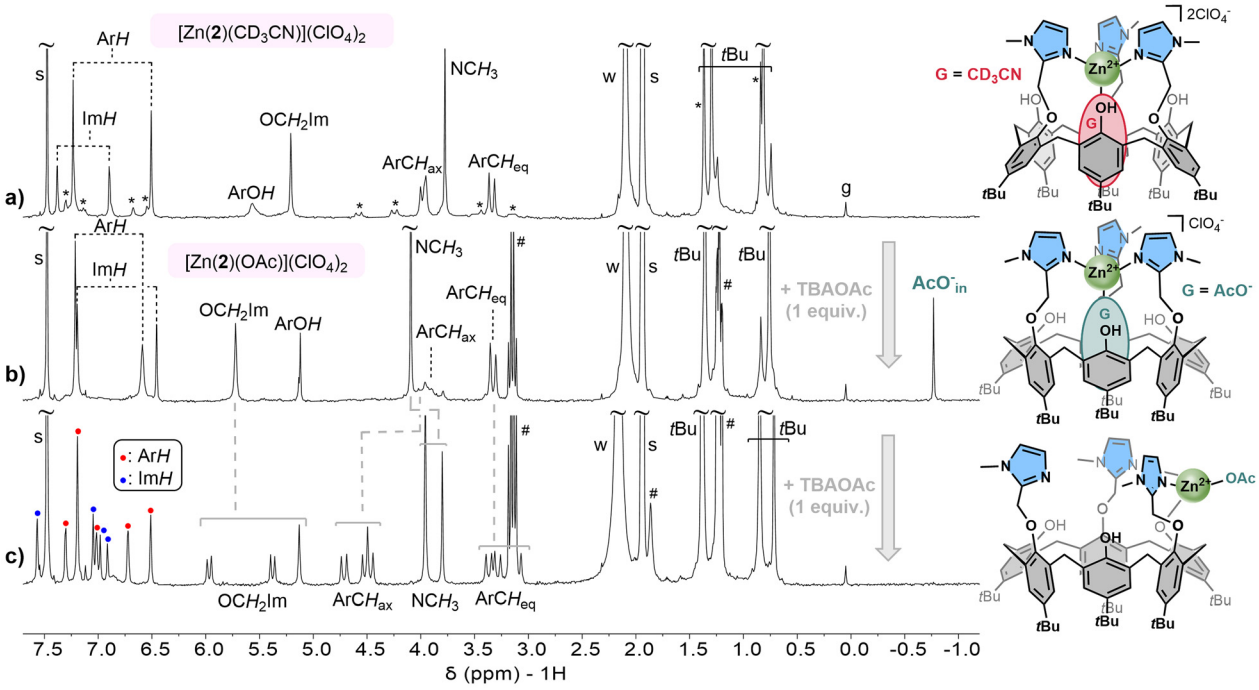

Fig. 5 ^{1}H NMR spectra (298 K, 400 MHz, $CDCl_3/CD_3CN$ 1 : 1) of (a) $[Zn(\mathbf{2})(G)](ClO_4)_2$, (b) after addition of 1 equiv. of TBAOAc and (c) after addition of a total amount of 2 equiv. of TBAOAc. *: minor conformer. #: TBA and AcOH.

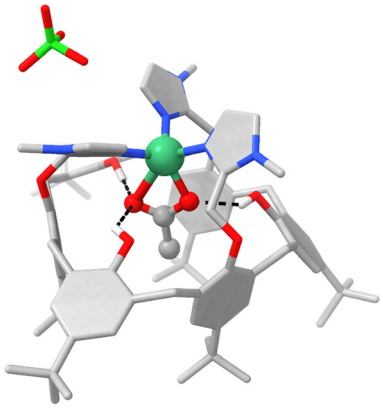

Fig. 6 X-ray diffraction structure of [Zn(**2**)(OAc)](ClO_4). H-bonds are indicated by black dashed lines.

two oxygen atoms of the carboxylate [d(O–O) = 2.71, 2.72 and 2.95 Å]. Consequently, the remaining perchlorate anion is not involved in H-bonding interaction with the phenol groups.

The third species formed upon the addition of 2 equiv. of acetate was characterized using additional NMR experiments (Fig. 5c and S37–S41). The ^{1}H NMR spectrum closely resembles those obtained with an excess of equiv. of propylamine and DBU, and is consistent with the formation of a C_s-symmetrical complex. Variations in the chemical shifts of some resonances (for instance for the two doublets and the singlet for the OCH_2Im protons) are likely due to the different nature of the fourth ligand occupying the *exo*-coordination site: acetate, propylamine or DBU. The signal for the OH groups cannot be identified probably due to its broadness. Hence, after the stabilization of the first equivalent of acetate *via endo*-coordination and H-bonding interactions, the receptor is engaged in acid–base chemistry with the free acetate anions, leading to the deprotonation of one phenol unit, its coordination to the zinc cation and the *exo*-coordination of the acetate initially bound within the cavity (see structure in Fig. 5c).

The behaviour of [Zn(**3**)(CH_3CN)](ClO_4)$_2$ toward acetate was next investigated. Comparison with the spectra recorded for [Zn(**2**)(CH_3CN)](ClO_4)$_2$ advocate for the same behaviour in the presence of acetate (see SI section VII and Fig. S42–S51).

To further explore the interplay between anion recognition and acid–base reactivity, we probed the influence of the cavity size by using a longer carboxylate anion. A titration using an equimolar mixture of hexanoic acid and triethylamine revealed only signs of deprotonation and no evidence of recognition for [Zn(**2**)(CH_3CN)](ClO_4)$_2$, even before the addition of the first equivalent (Fig. S52 and S53), suggesting that deprotonation dominates over intra-cavity binding in this case. In contrast, with [Zn(**3**)(CH_3CN)](ClO_4)$_2$, the same titration led to the formation of the inclusion complex, even though the deprotonation of the complex, characterized by the broadening of the spectrum, was observed before the recognition of one equivalent of the carboxylate guest (Fig. S54 and S55). These results highlight the influence of the cavity size on the competition between binding and deprotonation.

We also assessed the importance of the second coordination sphere provided by the phenol units, using a pseudo-halide (N_3^-) or a halide (Cl^-) anion. Although azide has a pK_a similar to that of acetate (pK_a ≈ 4.7 in water for both anions), its linear geometry makes the dual stabilization by coordination to the zinc cation and H-bonding less favourable than for carboxylates. ^{1}H NMR titration of [Zn(**2**)(G)](ClO_4)$_2$ with tetrabutylammonium azide in $CDCl_3$/CD_3CN (1 : 1) led directly to the formation of a single new species, with no detectable intermediate (Fig. S56 and S57). The ^{1}H NMR spectrum of this complex is consistent with the previously observed C_s-symmetrical deprotonated complex formed in the presence of acetate, propylamine, or DBU (Fig. S58), but in this case featuring *exo*-coordination of the azide anion. Interestingly, the less basic chloride anion (pK_a ≈ −5.9 in water) seems to behave similarly to the azide anion, leading eventually to the deprotonation of the complex (Fig. S63).

Finally, a biphasic extraction experiment proved the ability of [Zn(**2**)(G)](ClO_4)$_2$ to extract acetate from an aqueous phase (see SI section XI and Fig. S64).

Discussion

In this study, we have compared three funnel complex receptors based on a calix[6]arene scaffold capped by a trisimidazolyl-Zn^{2+} unit with a labile coordination site located within the macrocyclic cavity. Two of these receptors are reported here for the first time. While they share a common design, they differ in the nature of their second coordination sphere (either three bulky methoxy groups or three H-bond donor OH groups) and their third coordination sphere, defined by the presence or absence of six *t*Bu substituents at the large rim of the calixarene (see inset in Fig. 1).

These structural differences enable to finely identify important parameters that govern the host–guest properties of this family of biomimetic receptors towards neutral and anionic guests:

(i) *Influence of the second coordination sphere on the binding of anions.* The nature of the second coordination sphere (OCH_3 *vs.* OH) determines whether the receptor selectivity binds only neutral guests or both neutral and anionic guests. The anisole-containing receptor does not interact with anions, due to its conformation, which orients the oxygen lone pairs of the OCH_2-imidazole units toward the binding site of the Zn cation, generating electrostatic repulsion toward anionic guests. Also, the OCH_3 groups are too bulky to pivot inside the cavity and prevent any conformational rearrangement required for anion binding. Replacing the methoxy groups with hydroxyl groups releases this steric constrain, enabling the necessary conformational change. This structural rearrangement cancels the electrostatic repulsion and reorients the phenol OH groups toward the cavity, allowing them to engage in H-bonding interactions with anionic guests. Similar behaviour has previously

been observed for second-generation funnel complexes capped with a TREN ligand, where substitution of OCH_3 with OH groups likewise enhanced anion binding properties.[53]

(ii) *Modulation of the selectivity for neutral guests by the nature of the second coordination sphere.* The anisole-containing receptor preferentially binds strong σ-donor neutral guests, such as primary amines, due to their high affinity for Zn^{2+}. In contrast, receptors presenting phenol units display a more refined selectivity: they distinguish basic (*e.g.* propylamine) and non-basic neutral guests (*e.g.* acetonitrile). In both solution and the solid state, acetonitrile binds to the metal center though the calixarene cavity. In contrast, primary amines induce a metal-assisted deprotonation of one phenol unit rather than forming an inclusion complex. The resulting phenolate anion coordinates to the Zn^{2+} center, pushing the metal ion away from the cavity and abolishing its affinity for intracavity guest recognition. This structural reorganization is confirmed by X-ray crystallography (Fig. 4).

(iii) *Modulation of the selectivity for basic neutral guests by the nature of the first coordination sphere.* Interestingly, the [Zn(**Calix-TREN^{H}**)] receptor behaves differently: the recognition of propylamine is still favored ($K_a = 6 \times 10^3$ M^{-1}) over the deprotonation of a phenol unit, as found for $[Zn(\mathbf{2})(G)](ClO_4)_2$.[52] This comparison highlights the crucial role of the first coordination sphere in determining the binding properties of funnel complexes.

(iv) *Interplay between anion recognition and acid–base reactivity.* The entanglement between the recognition properties and the acid–base reactivity can be finely studied with the two new receptors reported herein, showing the importance of both the second coordination sphere defined by the OH groups of the phenols units and the third coordination sphere defined by the remote interaction imposed by the cavity of the calix[6]arene.

(v) *Role of the second coordination sphere.* In non protic organic solvents, acetate is more basic than primary amines (in CH_3CN, pK_a = 23.5 for $AcOH/AcO^-$ and pK_a = 18.4 for $PrNH_3^+/PrNH_2$).[55–57] Nevertheless, the first equivalent of acetate does not deprotonate the phenol as propylamine does, but binds within the cavity of the receptors. XRD analysis confirms that the acetate is coordinated to the Zn^{2+} and further stabilized by three H-bonds with the three phenol OH donors. These interactions make the recognition of the acetate thermodynamically more favorable than the deprotonation of a phenol. Interestingly, the azide anion, despite having a similar basicity than acetate and the less basic chloride anion cause the deprotonation of the receptor even under stoechiometric conditions. This difference between these anions is attributed to a better complementarity of the receptor with acetate. Indeed, the azide (or chloride), because of its linear (or spherical) shape and monodentate coordination mode, cannot, if coordinated to the Zn cation, benefit from the multiple H-bonding interactions with the phenol units, as the acetate does. The lack of these secondary interactions shifts the equilibrium toward phenol deprotonation rather than coordination.

(vi) *Role of the third coordination sphere.* In the funnel complexes, the first and second coordination spheres work in synergy with a third coordination sphere arising from the calix[6]arene cavity. This macrocyclic environment can sterically or electronically influence the binding and reactivity. The comparison between $[Zn(\mathbf{2})(G)](ClO_4)_2$ and $[Zn(\mathbf{3})(G)](ClO_4)_2$ in the presence of acetate does not shed any light on the role of the third coordination sphere, as this anion is fully embedded in both cases. However, using a longer carboxylate such as hexanoate highlights the role of the cavity's size. The alkyl chain is long enough to bump into the *t*Bu substituents present at the large rim, introducing some steric bulk that is not present when the *t*Bu groups are removed. The receptor with a closed cavity, *i.e.* $[Zn(\mathbf{2})(G)](ClO_4)_2$, shows no evidence of guest recognition but undergoes deprotonation instead. Conversely, the open-cavity receptor, *i.e.* $[Zn(\mathbf{3})(G)](ClO_4)_2$, accommodates the hexanoate guest, demonstrating that the third coordination sphere can modulate the accessibility and positioning of the guest, and ultimately control the receptor's reactivity.

Conclusion

We report on the synthesis and characterization of two new receptors that expand the family of Zn^{2+} funnel complexes featuring a tris-imidazole first coordination sphere. The NMR studies in solution and the XRD analyses in the solid state converge and give a clear picture of the respective role of the different coordination spheres in governing guest recognition within this family of receptors. In particular, the presence of the methoxy groups on the small rim, close to the intra-cavity metal coordination site, restricts the receptor's affinity to neutral guests such as nitriles or primary amines. The substitution of these methoxy groups with hydroxyl groups enables a conformational rearrangement, that, together with directional hydrogen bonding, enables selective recognition of anionic guests, while preserving affinity for non-basic neutral species. Recognition of basic species is strongly interlocked with the acid–base reactivity of the receptors presenting three phenol units. When the steric or electronic complementarity between the receptor and the basic guest is not optimal (*e.g.* unfavorable stabilization of the guest by H-bonds with the OH and/or steric clash between the *t*Bu substituents and a long alkyl chain), the receptor undergoes deprotonation, assisted by the Zn^{2+} center, thereby precluding further guest inclusion. Conversely, when the basic guest fits all structural and electronic criteria, acid–base reactivity is silenced in favor of stable complexation. Altogether, this study demonstrates that calix[6]arene-based metallo-receptors can be precisely tuned at multiple structural levels to modulate both selectivity and reactivity toward a wide range of guests. Their demonstrated ability to extract anions from aqueous media further positions them as promising candidates for applications in transmembrane transport,[58,59] ion sensing, or as molecular probes in micelles.[60]

Experimental section

Synthetic procedure

Synthesis of [Zn(2)(CH$_3$CN)](ClO$_4$)$_2$. To a mixture of ligand **2** (100 mg, 0.0796 mmol) dissolved in a solution of acetonitrile (0.5 mL) and chloroform (0.5 mL) was added Zn(ClO$_4$)$_2$·6H$_2$O (29.6 mg, 0.0796 mmol). The solution was then stirred for 1 hour. Diethyl ether (4 mL) was added to the reaction mixture and the resulting white precipitate was collected by centrifugation (5 min, 4000 rpm). The solid residue was dried under vacuum to afford [Zn(**2**)(CH$_3$CN)](ClO$_4$)$_2$ as a white powder (105 mg, 0.0689 mmol, 87%). Mp: >230 °C. IR: (CH$_3$CN) ν_{max}: 2980, 2360, 2252, 1442, 1377, 1037, 918. ^{1}H NMR (400 MHz, CD$_3$CN, 298 K): δ (ppm) 7.40 (s, 3H, Im*H*), 7.32 (s, 6H, Ar*H*), 6.93 (s, 3H, Im*H*), 6.51 (s, 6H, Ar*H*), 5.57 (s, 3H, ArO*H*), 5.23 (s, 6H, C*H*$_2$Im), 4.01 (d, J = 14.7 Hz, 6H, ArCH_{ax}), 3.75 (s, 9H, NC*H*$_3$), 3.37 (d, J = 14.7 Hz, 6H, ArCH_{eq}), 1.33 (s, 27H, *t*Bu), 0.81 (s, 27H, *t*Bu).^{13}C NMR (126 MHz, CD$_3$CN, 298 K): δ (ppm) 154.6, 148.9, 148.2, 143.3, 134.1, 133.3, 129.2, 128.5, 127.5, 125.4, 123.9, 65.2, 35.4, 35.0, 34.4, 31.7, 30.7. HRMS (SI) m/z: [M − 2ClO$_4^-$]$^{2+}$: Calcd for [C$_{81}$H$_{102}$O$_6$N$_6$Zn]$^{2+}$: 659.3571 found: 659.3554.

Synthesis of [Zn(3)(CH$_3$CN)](ClO$_4$)$_2$. To a mixture of ligand **3** (100 mg, 0.109 mmol) dissolved in a solution of acetonitrile (0.5 mL) and chloroform (0.5 mL) was added Zn(ClO$_4$)$_2$·6H$_2$O (40.5 mg, 0.109 mmol). The solution was then stirred for 1 hour. Diethyl ether (4 mL) was added to the reaction mixture and the resulting white precipitate was collected by centrifugation (5 min, 4000 rpm). The solid residue was dried under vacuum to afford [Zn(**3**)(CH$_3$CN)](ClO$_4$)$_2$ as a pale orange powder (116 mg, 0.0980 mmol, 90%). Mp: >230 °C. IR: (CH$_3$CN) ν_{max}: 2361, 2341, 1651, 1111. ^{1}H NMR (400 MHz, CDCl$_3$/CD$_3$CN 1 : 1, 298 K): δ (ppm) 7.36 (s, 3H, Im*H*), 7.29 (d, J = 7.5 Hz, 6H, Ar*H*), 7.20 (t, J = 7.5 Hz, 3H, Ar*H*), 6.80 (s, 3H, Im*H*), 6.31 (t, J = 7.5 Hz, 3H, Ar*H*), 6.18 (d, J = 7.5 Hz, 6H, Ar*H*), 5.92 (s, 3H, ArO*H*), 5.02 (s, 6H, C*H*$_2$Im), 3.91 (s, 6H, ArCH_{ax}), 3.62 (s, 9H, NC*H*$_3$), 3.43 (s, 6H, ArCH_{eq}).^{13}C NMR (126 MHz, CDCl$_3$/CD$_3$CN 1 : 1, 298 K) δ (ppm) 157.0, 150.8, 147.3, 133.1, 132.4, 127.8, 126.9, 125.7, 125.3, 125.2, 120.6, 63.9, 34.9, 31.1, 31.1, 30.9. HRMS (SI): m/z: [M − 2ClO$_4^-$]$^{2+}$: Calcd for [C$_{57}$H$_{54}$O$_6$N$_6$Zn]$^{2+}$: 491.1693 found: 491.1691.

Author contributions

I. J. and B. C. conceived and directed the project. M. L. performed the experiments. A. V. performed the XRD studies. I. J., B. C. and M. L. analysed the data. I. J., B. C. and M. L. wrote the paper. All authors discussed the results and commented on the manuscript.

Conflicts of interest

There are no conflicts to declare.

Data availability

The data supporting this article have been included as part of the SI.

General information, spectroscopic characterization data [1D and 2D NMR spectra (^{1}H, ^{13}C, COSY, HSQC, HMBC)]. The authors have cited additional references within the SI.[61–66] See DOI: https://doi.org/10.1039/d5ob01099c.

CCDC 2442673 (for [Zn(**2**)(OAc)](ClO$_4$)), 2442674 (for [Zn(**3**)(CH$_3$CN)](ClO$_4$)$_2$) and 2442675 (for [Zn(**3**)(CH$_3$CN)](ClO$_4$)$_2$) contain the supplementary crystallographic data for this paper.[67a–c]

Acknowledgements

This research was supported by the Fonds pour la formation à la Recherche dans l'Industrie et dans l'Agriculture (FRIA-FRS, Belgium), the Agence Nationale pour la Recherche (Marcel Project ANR-21-CE50-0034-02) and by the Croatian Science Foundation (grant: IP-2020-02-3786, PI: A. Višnjevac). We thank the Centre d'Instrumentation en Resonance Magnétique – CIREM (Université libre de Bruxelles – ULB, Belgium) for providing support and access to its infrastructure, the NMR spectrometers used in this work have been funded by the Fonds de la Recherche Scientifique (F.R.S.-FNRS – FRFC-2.4.517.05 and LN-9.4501.98) and ULB. The authors thank Dr Nicola Demitri from the Elettra-Sincrotrone Trieste S.C.p.A for the data collection on one sample.

References

1 L. Pauling, *Nature*, 1948, **161**, 707.
2 I. H. Williams, *Beilstein J. Org. Chem.*, 2010, **6**, 1026.
3 R. Suno, *J. Biochem.*, 2024, **175**, 357.
4 A. W. Kahsai, K. S. Shah, P. J. Shim, M. A. Lee, B. N. Shreiber, A. M. Schwalb, X. Zhang, H. Y. Kwon, L.-Y. Huang, E. J. Soderblom, S. Ahn and R. J. Lefkowitz, *Proc. Natl. Acad. Sci. U. S. A.*, 2023, **120**, e2303794120.
5 V. R. Mingione, Y. Paung, I. R. Outhwaite and M. A. Seeliger, *Biochem. Soc. Trans.*, 2023, **51**, 373.
6 E. Persch, O. Dumele and F. Diederich, *Angew. Chem., Int. Ed.*, 2015, **54**, 3290.
7 S. Z. Vatsadze, A. L. Maximov and V. I. Bukhtiyarov, *Dokl. Chem.*, 2022, **502**, 1.
8 M. J. Wilkinson, P. W. N. M. van Leeuwen and J. N. H. Reek, *Org. Biomol. Chem.*, 2005, **3**, 2371.
9 C. M. Hong, R. G. Bergman and K. N. Raymond, *Acc. Chem. Res.*, 2018, **51**, 2447.
10 P. Liu, F. Fang, H. Wang and N. M. Khashab, *Angew. Chem., Int. Ed.*, 2023, **62**, e202218706.
11 N. Busschaert, C. Caltagirone, W. Van Rossom and P. A. Gale, *Chem. Rev.*, 2015, **115**, 8038.
12 S. Sarkar, P. Ballester, M. Spektor and E. A. Kataev, *Angew. Chem., Int. Ed.*, 2023, **62**, e202214705.

13 Y. Saylan, Ö. Erdem, F. Inci and A. Denizli, *Biomimetics*, 2020, **5**, 20.
14 A. P. Davis, *Chem. Soc. Rev.*, 2020, **49**, 2531.
15 G. Picci, R. Montis, V. Lippolis and C. Caltagirone, *Chem. Soc. Rev.*, 2024, **53**, 3952.
16 Q.-H. Ling, Z.-C. Lou, L. Zhang, T. Jin, W.-T. Dou, H.-B. Yang and L. Xu, *Chem. Soc. Rev.*, 2024, **53**, 6042.
17 J. T. Davis, P. A. Gale and R. Quesada, *Chem. Soc. Rev.*, 2020, **49**, 6056.
18 D. Das, K. I. Assaf and W. M. Nau, *Front. Chem.*, 2019, **7**, 619.
19 L. A. Marchetti, L. K. Kumawat, N. Mao, J. C. Stephens and R. B. P. Elmes, *Chem*, 2019, **5**, 1398.
20 Y.-C. Pan, X.-Y. Hu and D.-S. Guo, *Angew. Chem., Int. Ed.*, 2021, **60**, 2768.
21 J. Lagona, P. Mukhopadhyay, S. Chakrabarti and L. Isaacs, *Angew. Chem. Int. Ed.*, 2005, **44**, 4844, (*Angew. Chem.*, 2005, **117**, 4922).
22 J. Szejtli, *Chem. Rev.*, 1998, **98**, 1743.
23 Y. Yu, J. Yang and J. Rebek, *Chem*, 2020, **6**, 1265.
24 Y. Zhu, M. Zhao, J. Rebek and Y. Yu, *ChemOpen*, 2022, **11**, e202200026.
25 P. Timmerman, W. Verboom and D. N. Reinhoudt, *Tetrahedron*, 1996, **52**, 2663.
26 T. Ogoshi and T. Yamagishi, *Eur. J. Org. Chem.*, 2013, 2961.
27 T. Ogoshi, S. Kanai, S. Fujinami, T. Yamagishi and Y. Nakamoto, *J. Am. Chem. Soc.*, 2008, **130**, 5022.
28 M. Xue, Y. Yang, X. Chi, Z. Zhang and F. Huang, *Acc. Chem. Res.*, 2012, **45**, 1294.
29 C. D. Gutsche, in *Calixarenes: An Introduction*, ed. J. F. Stoddart, The Royal Society of Chemistry, Cambridge, 2nd edn, 2008.
30 J. Pfeuffer-Rooschüz, L. Schmid, A. Prescimone and K. Tiefenbacher, *JACS Au*, 2021, **1**, 1885.
31 K. Hermann, Y. Ruan, A. M. Hardin, C. M. Hadad and J. D. Badjić, *Chem. Soc. Rev.*, 2015, **44**, 500.
32 L. Escobar and P. Ballester, *Chem. Rev.*, 2021, **121**, 2445.
33 R. Z. Pavlović, Z. Lei, T. J. Finnegan, C. A. Waudby, X. Wang, V. W. L. Gunawardana, X. Zhu, C. M. Wong, T. Hamby, C. E. Moore, N. Hoefer, D. W. McComb, C. S. Sevov and J. D. Badjić, *Angew. Chem., Int. Ed.*, 2022, **61**, e202211304.
34 D. Diao, A. J. Simaan, A. Martinez and C. Colomban, *Chem. Commun.*, 2023, **59**, 4288.
35 J.-N. Rebilly, B. Colasson, O. Bistri, D. Over and O. Reinaud, *Chem. Soc. Rev.*, 2015, **44**, 467.
36 R. Gramage-Doria, D. Armspach and D. Matt, *Coord. Chem. Rev.*, 2013, **257**, 776.
37 J. L. Atwood, L. J. Barbour and A. Jerga, *Proc. Natl. Acad. Sci. U. S. A.*, 2002, **99**, 4837.
38 J. T. Lenthall and J. W. Steed, *Coord. Chem. Rev.*, 2007, **251**, 1747.
39 M. Guitet, P. Zhang, F. Marcelo, C. Tugny, J. Jiménez-Barbero, O. Buriez, C. Amatore, V. Mouriès-Mansuy, J.-P. Goddard, L. Fensterbank, Y. Zhang, S. Roland, M. Ménand and M. Sollogoub, *Angew. Chem., Int. Ed.*, 2013, **52**, 7213.
40 M. Zhao, H.-B. Wang, L.-N. Ji and Z.-W. Mao, *Chem. Soc. Rev.*, 2013, **42**, 8360.
41 R. Lavendomme, S. Zahim, G. De Leener, A. Inthasot, A. Mattiuzzi, M. Luhmer, O. Reinaud and I. Jabin, *Asian J. Org. Chem.*, 2015, **4**, 710.
42 P. Neri, J. L. Sessler and M.-X. Wang, *Calixarenes and Beyond*, Springer, Cham, 2017.
43 N. Le Poul, Y. Le Mest, I. Jabin and O. Reinaud, *Acc. Chem. Res.*, 2015, **48**, 2097.
44 Y. Rondelez, M.-N. Rager, A. Duprat and O. Reinaud, *J. Am. Chem. Soc.*, 2002, **124**, 1334.
45 D. Coquière, S. Le Gac, U. Darbost, O. Sénèque, I. Jabin and O. Reinaud, *Org. Biomol. Chem.*, 2009, **7**, 2485.
46 D. Coquière, A. de la Lande, S. Martí, O. Parisel, T. Prangé and O. Reinaud, *Proc. Natl. Acad. Sci. U. S. A.*, 2009, **106**, 10449.
47 O. Sénèque, M.-N. Rager, M. Giorgi and O. Reinaud, *J. Am. Chem. Soc.*, 2000, **122**, 6183.
48 U. Darbost, M.-N. Rager, S. Petit, I. Jabin and O. Reinaud, *J. Am. Chem. Soc.*, 2005, **127**, 8517.
49 N. Le Poul, B. Douziech, J. Zeitouny, G. Thiabaud, H. Colas, F. Conan, N. Cosquer, I. Jabin, C. Lagrost, P. Hapiot, O. Reinaud and Y. Le Mest, *J. Am. Chem. Soc.*, 2009, **131**, 17800.
50 A. Brugnara, F. Topić, K. Rissanen, A. de la Lande, B. Colasson and O. Reinaud, *Chem. Sci.*, 2014, **5**, 3897.
51 P.-E. Danjou, G. De Leener, D. Cornut, S. Moerkerke, S. Mameri, A. Lascaux, J. Wouters, A. Brugnara, B. Colasson, O. Reinaud and I. Jabin, *J. Org. Chem.*, 2015, **80**, 5084.
52 G. De Leener, D. Over, O. Reinaud and I. Jabin, *Org. Biomol. Chem.*, 2023, **21**, 1172.
53 P. Aoun, N. Nyssen, S. Richard, F. Zhurkin, I. Jabin, B. Colasson and O. Reinaud, *Chem. – Eur. J.*, 2023, **29**, e202202934.
54 M. Lepeintre, J. Champiaux, B. Colasson and I. Jabin, *J. Org. Chem.*, 2024, **89**, 4210.
55 E. Raamat, K. Kaupmees, G. Ovsjannikov, A. Trummal, A. Kütt, J. Saame, I. Koppel, I. Kaljurand, L. Lipping, T. Rodima, V. Pihl, I. A. Koppel and I. Leito, *J. Phys. Org. Chem.*, 2013, **26**, 162.
56 A. Kütt, S. Tshepelevitsh, J. Saame, M. Lõkov, I. Kaljurand, S. Selberg and I. Leito, *Eur. J. Org. Chem.*, 2021, 1407.
57 S. Tshepelevitsh, A. Kütt, M. Lõkov, I. Kaljurand, J. Saame, A. Heering, P. G. Plieger, R. Vianello and I. Leito, *Eur. J. Org. Chem.*, 2019, 6735.
58 G. Grauwels, H. Valkenier, A. P. Davis, I. Jabin and K. Bartik, *Angew. Chem., Int. Ed.*, 2019, **58**, 6921.
59 N. Renier, O. Reinaud, I. Jabin and H. Valkenier, *Chem. Commun.*, 2020, **56**, 8206.
60 E. Brunetti, A. Inthasot, F. Keymeulen, O. Reinaud, I. Jabin and K. Bartik, *Org. Biomol. Chem.*, 2015, **13**, 2931.
61 CrysAlis CCD, *Version 1.171.32.29 (release 10–02008 CrysAlis171.NET)*, Oxford Diffraction Ltd.
62 U. Mueller, M. Thunnissen, J. Nan, M. Eguiraun, F. Bolmsten, A. Milàn-Otero, M. Guilarro, M. Oscarsson,

D. de Santis and G. Leonard, *Synchrotron Radiat. News*, 2017, **30**, 22.
63 W. Kabsch, *Acta Crystallogr., Sect. D:Biol. Crystallogr.*, 2010, **66**, 125.
64 G. M. Sheldrick, *Acta Crystallogr., Sect. A:Found. Adv.*, 2015, **71**, 3.
65 G. M. Sheldrick, *Acta Crystallogr., Sect. B:Struct. Sci., Cryst. Eng. Mater.*, 2015, **71**, 3.
66 O. V. Dolomanov, L. J. Bourhis, R. J. Gildea, J. A. K. Howard and H. Puschmann, *J. Appl. Crystallogr.*, 2009, **42**, 339.
67 (*a*) M. Lepeintre, A. Višnjevac, I. Jabin and B. Colasson, CCDC 2442673: Experimental Crystal Structure Determination, 2025, DOI: **10.5517/ccdc.csd.cc2mzsxb**; (*b*) M. Lepeintre, A. Višnjevac, I. Jabin and B. Colasson, CCDC 2442674: Experimental Crystal Structure Determination, 2025, DOI: **10.5517/ccdc.csd.cc2mzsyc**; (*c*) M. Lepeintre, A. Višnjevac, I. Jabin and B. Colasson, CCDC 2442675: Experimental Crystal Structure Determination, 2025, DOI: **10.5517/ccdc.csd.cc2mzszd**.